20 Lecture 20. Lorenz system: Advanced topics

20.1 Knotted orbits[190,191]

Periodic orbits need not be without any knot. The Lorenz model exhibits tons of such orbits.[192]

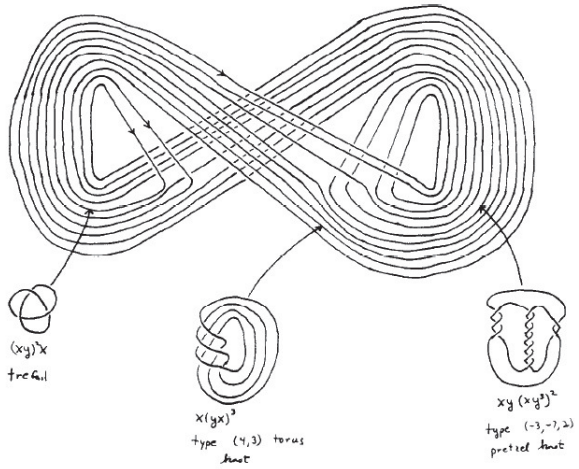

Figure 20.1: Schematic representation of coexisting knotted orbits [Fig. 1.1 of BIRMAN and WILLIAMS, Topology 22 47 (1983)]

Theorem [Franks and Williams][193]A smooth flow on S^3 with positive topological entropy[194] must possess periodic closed orbits in infinitely many different knot type equivalence classes.

Actually, Ghrist[195] proved that there is a structurally stable flow on S^3 that con-

[190]⟪**Knot**⟫ A knot is am embedding of S^1 into $\mathbb{R}^3$. It is knotted if the image is not homotopic to S^1.

[191]Incidentally, if a protein is stretched by pulling both the ends in th opposite direction, generally, the resultant polypeptide chain should be knotted. It is known that actually, knotted proteins are very rare.

[192]JOAN S. BIRMAN and R. F. WILLIAMS, KNOTTED PERIODIC ORBITS IN DYNAMICAL SYSTEMS I: LORENZ'S EQUATIONS, Topology 22 47 (1983).

[193]J. Franks and R. F. Williams, Entropy and knots, TAMS 291 241 (1985).

[194]Topological entropy is, practically, the largest KS entropy allowed to the system.

[195]R. Ghrist, Branched two-manifolds supporting all links, Topology 36 423 (1997).

tains all knot types as periodic orbits.

If the Lorenz system is periodically perturbed, we can even have links of periodic orbits.[196]

20.2 Geometrical Lorenz model[197]

A very fruitful approach was undertaken, independently, by V. Afraimovich, V. Bykov, L. Shirnikov [2], and by J. Guckenheimer and R. Williams [3, 4]. Based on the behavior observed in the previous Lecture (Fig. 20.2 Leftmost[198]), they exhibited a list of geometric properties such that any flow satisfying these properties must contain a "strange attractor,"[199] with orbits converging to it being sensitive to initial conditions. Most important for the general theory, they proved that such flows do exist in any manifold with dimension 3. These examples came to be known as geometric Lorenz models.

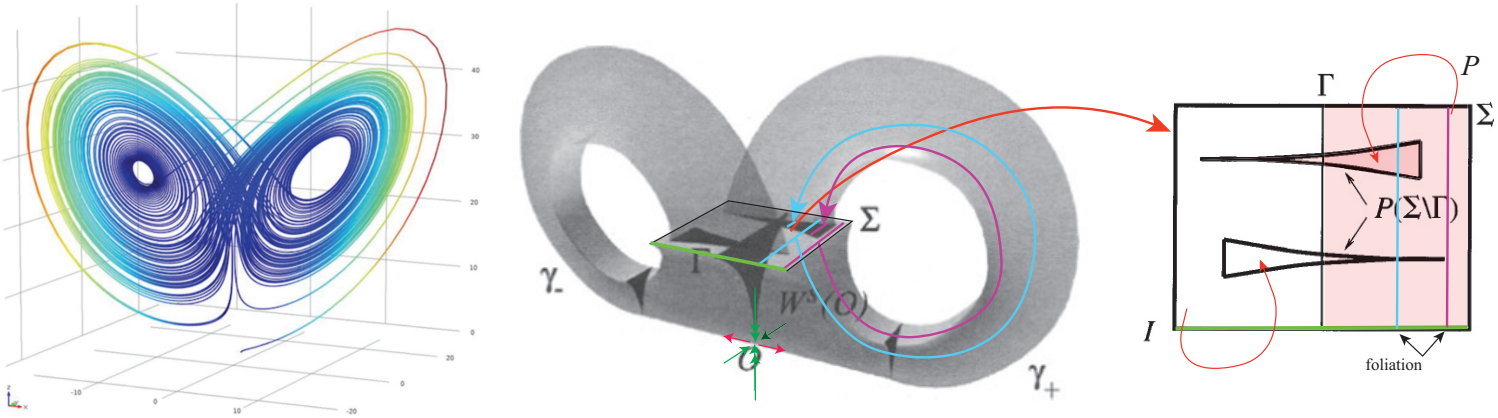

Figure 20.2: Geometric Lorenz model. The return map P maps $\Sigma \setminus \Gamma$ to Σ. I is the bottom segment (the green segment) of Σ. [Fig. 6, 8 of Viana Math Intel. 22(3) 7 (2000)]

In the above figure $\gamma_\pm$ (and $\{O\}$ (fixed point)) combined is the unstable manifold. The vertical direction is the (strong) stable direction. The weak stable direction is

[196] Y. Aizawa and T. Uezu, Topological aspects in chaos and in 2^k-period doubling cascade, Prog. Theor. Phys. 67 982 (1982).

[197] M Viana, "What's new on Lorenz strange attractors?" Math Intel. 22(3) 7 (2000).

[198] From https://ubisafe.org/explore/attractor-clipart-lorenz-attractor/.

[199] Here, the word is merely used to indicate an attracting set containing non-periodic orbits.

orthogonal to these manifolds. The stable manifold is spanned by these stable directions close to O.

The cross section is in the right of Fig. 20.2. We can define a return map P which is strongly contracting because of (19.14).

For the geometrical model, also the following foliation is assumed for P: Σ is foliated roughly transversally to I such that P is compatible with the foliation. That is, if z and z' ($\neq z$) are on the same leaf, so are $P(z)$ and $P(z')$. Furthermore, the distance between $P^k(z)$ and $P^k(z')$ shrinks to zero as $k \to \infty$. This means a leaf γ_1 is mapped inside some leaf γ_2. Since we can specify a leaf by its 'x' coordinate of the crossing point with I, P defines a map f from I into itself: $f : I \to I$. We assume

$$|f(x) - f(x')| \geq \tau |x - x'| \tag{20.1}$$

with $\tau > 1$. The graph of f looks like Fig. 20.3 (cf. Fig. 18.11).

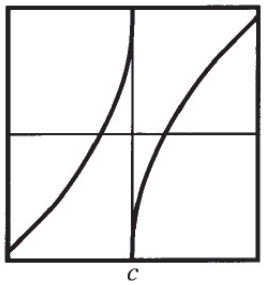

Figure 20.3: Interval maps related to the geometrical Lorenz model. Recall Fig. 18.11. [Fig. 10 of Viana Math Intel. 22(3) 7 (2000)]

The existence of a strange attractor containing O was proved for the geometric model. It has a topologically transitive orbit (if $\tau > \sqrt{2}$).

[1] V. S. Afraimovich, V. V. Bykov, and L. P. Shil'nikov. On the appearance and structure of the Lorenz attractor. Dokl. Acad. Sci. USSR, 234 336 (1977).

[2] J. Guckenheimer and R. F. Williams. Structural stability of Lorenz attractors. Publ. Math. IHES, 50 59-72 (1979).

[3] R.F. Williams. The structure of the Lorenz attractor. Publ Math. IHES, 50 73 (1979).

20.3 Lorentz attractor exists[200]

Theorem [Tucker 1998] For the classical parameters, the Lorenz equations (19.12)

[200] W. Tucker, The Lorenz attractor exists. PhD thesis, Univ. Uppsala, 1998. Text and program codes available at www.math.uu.se/~warwic/.; W. Tucker, The Lorenz attractor exists. C. R. Acad. Sci. Paris, 328, Serie I, Mathematique: 1197-1202 (1999).

support a robust strange attractor.

Tucker's computer-assisted proof is a combination of two main ingredients:[201]
(I) He uses rigorous numerics to find a cross-section Σ and a region N in Σ such that orbits starting in N always return to it in the future. After choosing reasonable candidates, Tucker covers N with small rectangles, as in Figure 20.4, and estimates the forward trajectories of these rectangles numerically, until they return to Σ. His computer program also provides rigorous bounds for the integration errors, good enough so that he can safely conclude that all of these rectangles return inside N. This proves that the equations do have some sort of attractor.

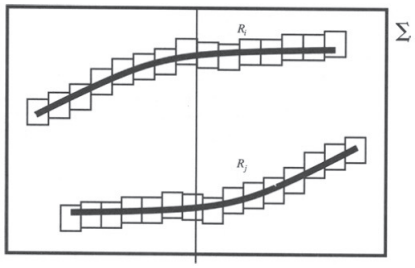

Figure 20.4: Attractor construction by Tucker [Fig. 4 of of Viana Math Intel. 22(3) 7 (2000)]

(II) Normal form theory comes in to avoid the accumulation of integration errors when trajectories are close to the equilibrium sitting at the origin.

20.4 Pseudo-orbit tracing property[202]

Here we consider a map $T : M \to M$, where M is a metric space. $\{x_n\}$ is a δ-pseudo-orbit if

$$\|Tx_n - x_{n+1}\| < \delta. \tag{20.2}$$

We say the orbit $\{T^n x\}$ ε-traces the pseudo-orbit $\{n_n\}$, if

$$\|T_n y - x_n\| < \varepsilon. \tag{20.3}$$

We say T has a pseudo-orbit tracing property (POTP), if for any ε (> 0) we can find δ (> 0) such that δ-pseudo-orbit can be ε-traced by an orbit $\{T^n y\}$.

[201] M Viana, "What's new on Lorenz strange attractors?" Math Intel. 22(3) 7 (2000).

[202] There is a general theorem that only the B systems can have POTP. That is, only if the system is very chaotic, POTP holds. [A necessary and sufficient condition for a system to have POTP is that it is isomorphic to a Markov subshift (Kubo Th 3.16). A Markov subshift is isomorphic to a Bernoulli shift (essentially the Ornstein theorem to be discussed later).]

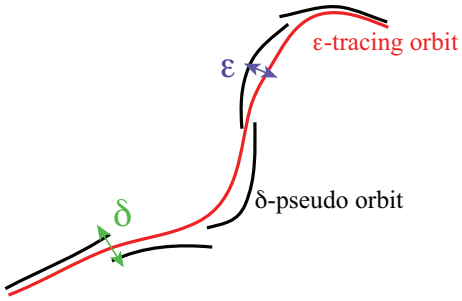

Figure 20.5: A pseudo orbit with a tracing property

This property is practically important. Pseudo-orbit tracing property implies that for a numerically obtained orbit with error δ there is a true orbit close to it for all time. If a system lacks POTP, then it is questionable that numerical simulation can always tell something correct about the system.

POTP for continuous dynamical system can be defined similarly (actually, the illustration in Fig. 20.5 is for this case).

We know chaotic billiards have POTP. Thus, if you make a reasonable numerical simulation, there is a true orbit starting somewhere. However, POTP never guarantees that pseudo orbits correctly sample the true orbits, so if you are interested in the statistical behavior of chaotic systems, you must not rely on POTP.

20.5 Lorenz system is not ε-traceable

The precise statement is that the geometrical Lorenz model lacks POTP. This is proved by showing the map $f : I \to I$ defined in **20.2** lacks POTP. f satisfies (see Fig. 20.3)

$$f(c+0) = 0, f(c-0) = 1, \tag{20.4}$$
$$f' > \lambda \geq 1, \tag{20.5}$$
$$f(0) < c < f(1), \tag{20.6}$$
$$\lim_{x \to c} f'(x) \to \infty. \tag{20.7}$$

Theorem [Komuro][203] $f : I \to I$ has the POTP if and only if $f(0) = 0$ and $f(1) = 1$.

The above theorem means that

[203] M. Komuro, Lorenz attractor do not have the pseudo-orbit tracing property, J Math Soc Jpn 37 489 (1985).

Theorem. Let M be a 3-dimensional compact manifold. Then the set of vector fields with the strong[204] POTP is not dense in $\mathcal{X}^2(M)$.

It is worth noting the following empirical fact. Usually, if a system exhibits 'chaotic behavior' in a certain parameter range, increasing the numerical accuracy in simulating the system shrinks the chaotic parameter range. The Lorenz system is known to be the opposite (at least in certain parameter ranges).[205]

20.6 Lorenz template

A template is the union of strips, and each strip is a copy of the standard 2-flow box $[0,1]\times[0,1]$ with flow parallel to the z edge. Where the strips meet, along branches, the vectors coincide so that a unique semi-flow is determined. The copying homeomorphism stretches the $x = 1$ end so that the resulting flow, where defined, is expanding. Two or more of these strips are assembled into a template, so that the resulting flow is well defined in the positive direction(, but at the branches it is not well defined for the negative time direction).[206]

An example is the Lorenz template (Fig, 20.6). We can understand the periodic orbits of the Lorenz system.

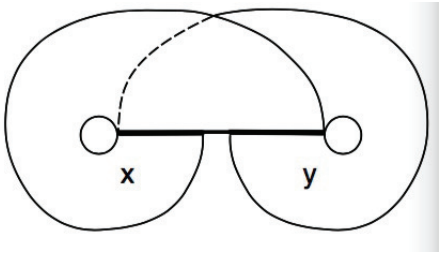

Figure 20.6: Lorenz template [Fig. 2 of Williams BAMS 35 145 (1998)]

In figure 20.6, the template consists of two strips, x and y, so that the flow on the left side passes around to the left and back down to the branch. Similarly, the flow on the right passes around to the right behind the strip x and back down to the branch. There is a middle portion at each branch, called a gap, at which the orbits leave the template. Orbits which leave are no longer of interest to us. Note that the periodic orbits never leave. The dark horizontal line is a branch; above it two planar

[204] For time continuous systems monotone time variable change is also allowed for the definition of POTP. If this time 'dilation is restricted to the scale range between $1 \pm \varepsilon$ globally, we say it is the strong POTP. Thus, numerically, we need strong POTP.

[205] M. Komuro, private communication (1979).

[206] R. F. Williams, The universal template of Ghrist, Bull AMS 35 145 (1998).

pieces come together where they are tangent to each other. Thus each point on a branch lies in two smooth disks which coincide below the branch, but are disjoint above. Each branch in a template is homeomorphic to the unit interval [0,1] and called a branch line.

As can be seen from Fig. 18.10, if there is no gap, the Lorenz template is exactly the spiral figure in this figure. For example, there is a one-to-one correspondence between periodic orbits of the two templates.

20.7 Shimada's Ising representation of Lorenz attractor[207]

The Lorenz attractor has two wings, so one rotation in one wing is assigned +1 spin and the other −1 to code the sequence. Since the orbits are deterministic, this coding may be interpreted as the coding of the initial position:

$$x \to s_1 s_2 \cdots, s_n \cdots, \quad \text{where } s_i \in \{-1, 1\}. \tag{20.8}$$

This map can also be understood as a map from x to $b \in [0, 1]$, if we regard (−1 as 0 and +1 as 1 and read the sequence as the binary expansion of a number in $[0, 1]$)

$$b = \sum_{k=1}^{\infty} \left(\frac{s_k + 1}{2} \right) 2^{-k}. \tag{20.9}$$

This is illustrated in Fig. 20.7

The spin configuration converges to a stationary distribution (Fig. 20.8 Left) which exhibits a self-similar structure due to the translational symmetry (time-stationarity) of the original system and the coding scheme. We can construct a 1D Ising Hamiltonian to reproduce this distribution as

$$H = -\sum_{i,j} J(|i - j|) s_i s_j. \tag{20.10}$$

The coupling constant decays exponentially as in Fig.20.8Right.

The entropy per spin mus t be the KS entropy of the Poincarémap . The latter may be estimated from the expansion rate of the nearby orbits (= Lyapunov characteristic number; we will discuss later). Numerically, Shimada confirmed the agreement.

[207] I Shimada, Gibbsian distribution on the Lorenz attractor," Prog Theor Phys 62 61 (1979).

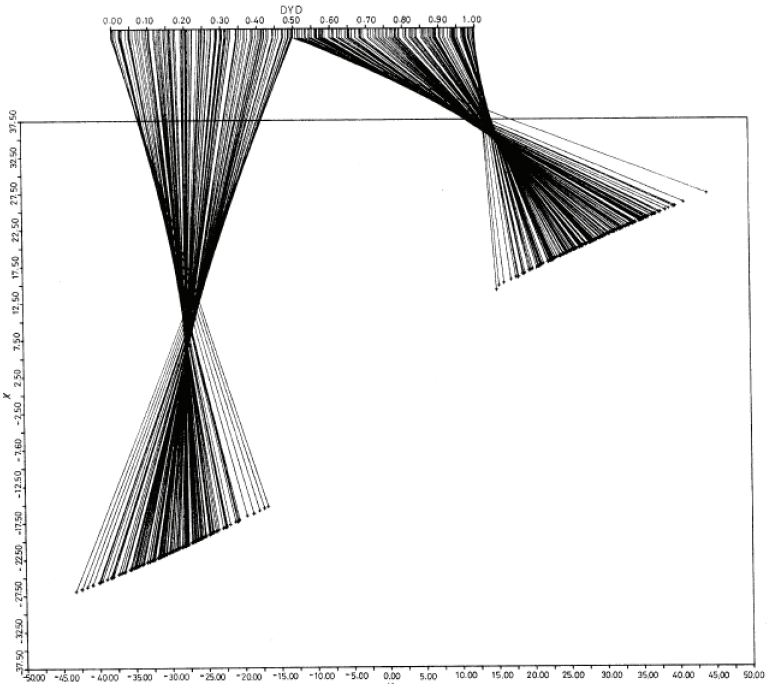

Figure 20.7: Correspondence $x \to b$ [Fig. 1 of Shimada PTP 62 61 (1979)]

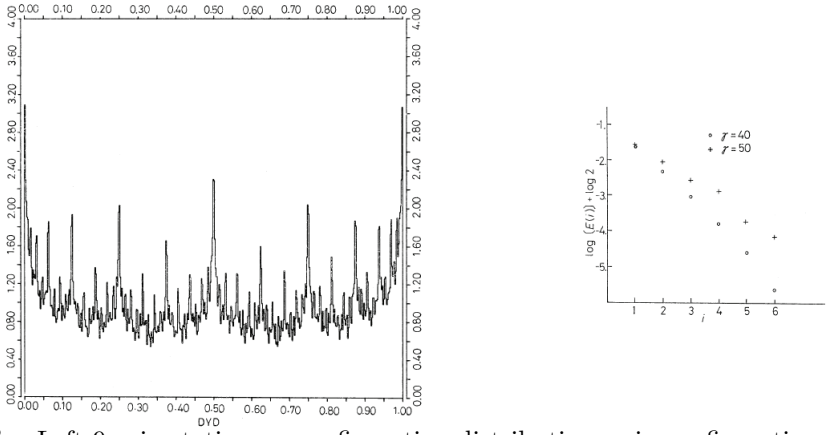

Figure 20.8: Left 9 spin stationary configuration distribution; spin configurations are described as b. Right: The coupling constant corresponding to the configurations (γ is our r) [Fig. 2 of Shimada PTP 62 61 (1979)]

20.8 Galerkin method

Reduction of PDE to a finite number of coupled ODEs may be very useful numerically as well as summarizing the system behavior in a finite dimensional space. A popular strategy is to use an appropriate orthogonal function set.

Consider a functional equation in a 'spatial domain' D:

$$\frac{d}{dt}u = N[u], \tag{20.11}$$

where N is a general nonlinear operator that can contain spatial derivatives. Take an appropriate orthonormal basis $\mathcal{B} = \{\phi_n(x)\}$ (assumed as a real function set) for the set of functions on D (considered as a Hilbert space). Expand u as

$$u(t,x) = \sum_j c_j(t)\phi_j(x), \tag{20.12}$$

and introduce it into (20.11)

$$\sum_j \frac{\partial c_j}{\partial t}\phi_j(x) = N\left[\sum_j c_j(t)\phi_j(x)\right]. \tag{20.13}$$

Then, project this onto ϕ_k:

$$\frac{\partial c_k}{\partial t} = \int_D dx\, \phi_k(x) N\left[\sum_j c_j(t)\phi_j(x)\right]. \tag{20.14}$$

To make this system manageable, we choose a finite subset $\mathcal{B}'$ of $\mathcal{B}$. The resultant set of (generally nonlinear) ODEs defines a Galerkin approximation to (20.11).[208]

One practical approach is to Fourier expand physically convenient ON function set $\{\phi_k\}$ and use the result to compute (20.14). For example, Yahata used this method to reduce the Taylor flow problem to 32 dimensions.[209]

---

[208] This is related to the principal component analysis.

[209] H. Yahata, Temporal Development of the Taylor Vortices in a Rotating Fluid, PTP Supp 64 176 (1978); he chose the number of functions to reproduce experimental results (say, bifurcations given by Harry Swinney). Some people try to choose $\mathcal{B}'$ (or $\mathcal{B}$) to minimize the errors, but they actually use heavy numerical solutions. However, you might have to do this optimization for only one state (or a parameter set) of the system and could use the result for 'neighbor' states, so one-time heavy investment may pay.

20.9 Use of inertial manifold in conjunction with Galerkin method[210]

To be added (maybe).

[210] C. FOIAS, M. S. JOLLY, I. G. KEVREKIDIS, G. R. SELL and E. S. TITI, ON THE COMPUTATION OF INERTIAL MANIFOLDS PL A131 433 (1988).